

Poly(*p*-Phenylenediamine) as an Inhibitor for Mild Steel in Hydrochloric Acid Medium

S.S Abd El Rehim,^a S.M. Sayyah^b and R.E. Azooz^{b,*}

^a Chemistry Department, Faculty of Science, Ain Shams University, Abbassia, Cairo, Egypt.

^b Polymer Research Laboratory, Chemistry Department, Faculty of Science, Beni-Suef University, 62514 Beni-Suef, Egypt.

Received 7 March 2011; accepted 28 February 2012

Abstract

The corrosion behavior of mild steel (MS) in HCl solution containing various concentrations of electropolymerized P(*p*-phenylenediamine), P(pPD), has been investigated using weight loss and potentiodynamic polarization techniques. The data obtained from the two techniques are comparable and showed that the presence of P(pPD) in the acid solutions suppresses the corrosion rate of MS indicating that these polymers act as corrosion inhibitors (predominantly as anodic inhibitors). The inhibition efficiency (IE%) of the polymer enhances with increasing their concentrations and decrease with an increase in temperature. The inhibition occurs through adsorption and formation of barrier film on the metal surface which separates the metal from direct contact with the corrosive medium and hence protects the metal against the corrosion. The adsorption followed the Langmuir isotherm. The thermodynamic functions of the adsorption and dissolution processes were evaluated.

Keywords: corrosion; inhibition; protection efficiency; mild steel; Langmuir isotherm.

Introduction

The uniform corrosion is the main problem in using mild steel (MS) in acidic solution. To protect MS from acidic environment corrosion inhibitors or coatings are used.

The most effective factors for the inhibiting effects of organic polymers are: the electronegative atoms (such as, N, S, P, O, etc.), the unsaturated bonds (such as, double bonds or triple bonds, etc.), the plane conjugated systems including all kinds of aromatic cycles, molecular area and molecular weight of the inhibitor molecule [2- 10].

* Corresponding author. E-mail: re_azooz@yahoo.com

According to the type of inhibitor species (anodic or cathodic) and the nature of metal or alloy, adsorption may be chemical or physical adsorption. In many cases, the efficiency of an organic compound as an inhibitor is due to its adsorption on the metal surface forming a barrier layer which separates the metal from the corrosive media [10].

Some phenylenediamines are used as corrosion inhibitors of MS; p-phenylenediamine, pPD, as a monomer was found to be less effective compared with other isomers o- or/and m- phenylenediamine [11]. Also, poly phenylenediamines are used; P(oPD) with concentration 15 ppm gives inhibition efficiency (IE%) of 95% [12], P(pPD) with concentration 50 ppm gives inhibition efficiency (IE%) of 73% [13] and P(mPD) after 168 H give 80% efficiency [14].

In this paper we report the inhibitive action of an electro synthetic p(pPD) on corrosion of mild steel in HCl solutions. The inhibition has been evaluated by weight loss and potentiodynamic polarization measurements. It is also the purpose of this work to test the experimental data obtained from the two techniques with Langmuir isotherm at different temperatures, in order to determine the thermodynamic functions for the adsorption process.

Experimental

Chemicals

P(pPD) was obtained by the electropolymerized of reagent grade p-phenylenediamine (Merck- Darmstadt, Germany) in aqueous acidic HCl (Riedel-de-Haën, Germany) by cyclic voltammetry technique [12]. Characterization is done by using FTIR- spectroscopy, UV spectroscopy, TGA and element analysis. The proposed structure of this polymer using these tools is represented in Scheme (1). DMF were provided by El-Naser Pharmaceutical Chemical Company (Egypt).



Scheme 1. Structure of P(pPD).

Methodology

For the weight loss measurements, rectangular specimens of mild steel (MS) (wt. %: 98.5% Fe, 0.33% C, 0.24% Si, 0.52% Mn, 0.04% Cr and 0.02% S) of size 3 cm x 4 cm x 0.2 cm were used. The working electrode was polished mechanically with silicon carbide (SiC) belts, 200 to 600 grit (Buehler, Ltd.), and 1 μm α -alumina (Buehler, Ltd.), washed with distilled water, then with acetone, and finally with double distilled water and dried. The weight loss, expressed in mgcm^{-2} , was determined by weighing the cleaned samples before and after immersion in HCl solution for 1 h. Weight loss was determined in the absence or presence of various concentrations of P(pPD), which was prepared previously in the same manner as [12].

The UV-vis.- spectrum for P(pPD) (at room temperature in the range 200-900 nm using dimethylformamide as a solvent and reference) consists of the following absorption peaks:

$\lambda_{\max} = 290$ and 263 for $\pi-\pi^*$ transition;

$\lambda_{\max} = 312$ nm for polaron- π^* transition and;

$\lambda_{\max} = 440$ nm for π -polaron transition.

The IR-spectra, show the following bands:

$\nu_{\max} = 3415, 3150 \text{ cm}^{-1}$ for NH_2 stretching vibration or OH strong hydrogen bonded group in H_2O molecules of hydration in polymer;

$\nu_{\max} = 3015 \text{ cm}^{-1}$ for CH stretching vibration of aromatic amine:

$\nu_{\max} = 1115 \text{ cm}^{-1}$ for CH bending vibration of quinoid ring;

$\nu_{\max} = 1509 \text{ cm}^{-1}$ for CN stretching vibration of quinod;

$\nu_{\max} = 1288 \text{ cm}^{-1}$ for CN stretching vibration of radical cation;

$\nu_{\max} = 1509 \text{ cm}^{-1}$ for CN stretching vibration benzene ring.

A weighted 0.01g of polymer was dissolved in solution (DMF: H_2O mix (2:98 v/v)) to give a stock solution containing 100 ppm of inhibitor.

For polarization measurements, the electrolytic cell was filled with 100 mL of 1.0 M HCl solution. The working electrode (MS), auxiliary electrode (Platinum wire) and the Luggin- prob were introduced into the cell containing the test solution ($\text{H}_2\text{O}/\text{DMF}$ (98:2 v/v) and the polymer with different concentrations. Potentiodynamic polarization measurements were performed using the Potentiostat / Galvanostat Wenking PGS 95 connected with PC computer.

The working electrode is a MS specimen in the form of rod. The rod was weld from one side to a copper wire used for electrical connection. The rod was embedded in a glass tube and epoxy resin was used to stick the sample to the glass tube. This also ensured that a constant cross-section area of 2 cm^2 would be exposed to the solution through the experiments. The exposed area was ground by different emery papers in the normal way as described above, washed with distilled water, then with acetone, and again with distilled water, just before insertion in the cell. All the potentials were measured relative to the saturated calomel electrode (SCE). The i - E curves were recorded by computer software (Model ECT). For each run, a freshly prepared solution as well as a cleaned set of electrodes was used. Each run was conducted at constant temperature $\pm 1^\circ\text{C}$ with using a circular water thermostat.

P(pPD) [12] has the structure shown in scheme (1).~

Results and discussion

Weight loss and polarization measurements

The inhibition (protection) efficiency, $IE\%$, of P(pPD) was calculated for MS sample in the acid solutions in the presence of different concentrations of P(pPD) at 303 K using equation [13]:

$$IE\% = \left(1 - \frac{W}{W^0} \right) \times 100 \quad \text{Eq. (1)}$$

where, W^0 and W are the weight loss of MS sample in the absence and presence of P(pPD), respectively. The relation between $IE\%$ and the logarithm of the

concentration of the inhibitor in the three acid solutions at 303 K is shown in Fig. (1). From the figure, The P(pPD) species seems to function as inhibitor by being adsorbed on the metal surface from the corroding medium.

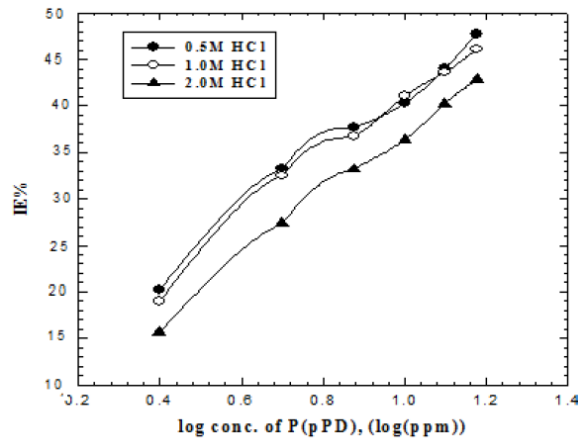


Figure 1. Relation between IE% and log of the concentration of P(pPD) in different HCl concentrations at 303 K.

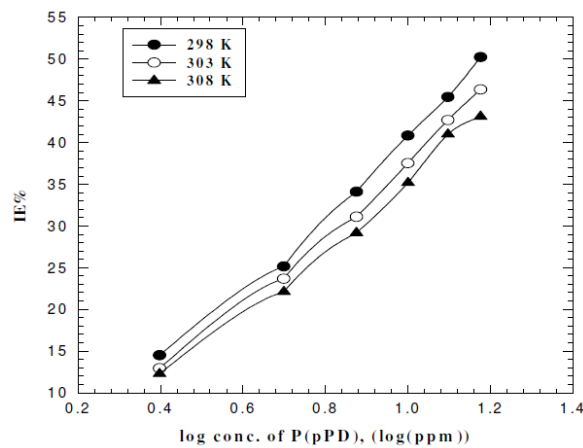


Figure 2. Relation between IE% and the log of the concentration of P(pPD) in 1.0 M HCl at 298, 303 and 308 K.

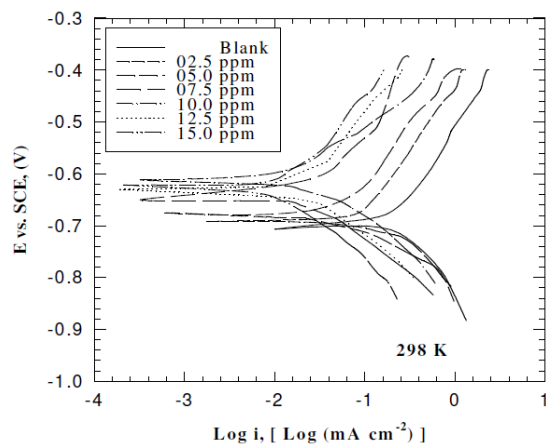


Figure 3. Effect of P(pPD) concentration on the potentiodynamic polarization curves of MS electrode in 1.0 M HCl at 298 K.

To verify the nature of adsorption and the effect of temperature on the corrosion behaviour of MS sample in 1 M HCl with and without different concentrations of P(pPD) inhibitor, weight loss studies were undertaken. The selected temperatures tested were 298, 303 and 308 K. The inhibition efficiency, IE%, under the prevailing conditions was calculated using equation (1) and the dependence of the IE% on the logarithm of the inhibitor concentration of P(pPD) at the three tested temperatures was shown in Fig. (2).

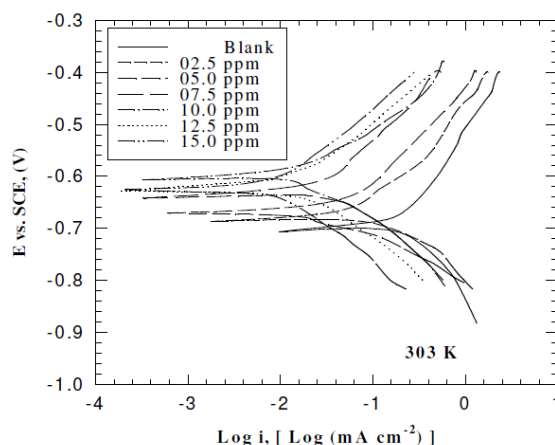


Figure 4. Effect of P(pPD) concentration on the potentiodynamic polarization curves of MS electrode in 1.0 M HCl at 303K.

From Fig. (1) and (2), one can conclude that the inhibition efficiency decrease with increasing the temperature. This can be due to the decrease in the strength of adsorption process at higher temperatures, suggesting that physical adsorption may be the type of adsorption of P(pPD) compound on MS sample surface. At a given temperature and inhibitor concentration, the inhibition efficiency decreases with increasing HCl concentration.

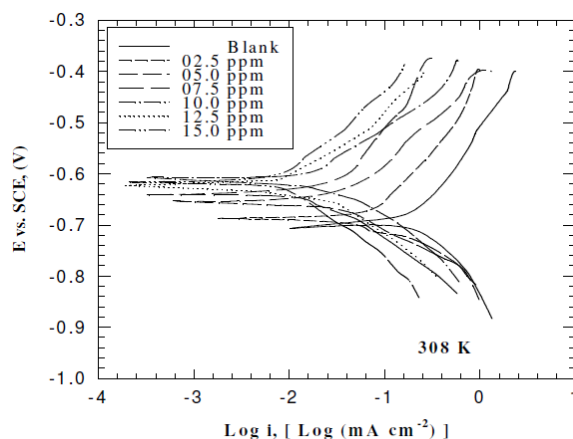


Figure 5. Effect of P(pPD) concentration on the potentiodynamic polarization curves of MS electrode in 1.0 M HCl at 308 K.

In order to get more information concerning the type of inhibitor, the nature of inhibition and the influence of the inhibitor on the kinetics of the partial cathodic and anodic reactions, potentiodynamic polarization curves have been conducted.

This was achieved by investigating the inhibitor concentration and solution temperature dependences of the corrosion current density (i_{corr}) and on the corrosion potential (E_{corr}), obtained using the Tafel extrapolation method.

Fig. (3), (4) and (5) represent the influence of P(pPD) concentration on the potentiodynamic cathodic and anodic polarization curves for MS electrode in 1.0 M HCl at scan rate of 10 mVs^{-1} and at 298, 303 and 308 K, respectively. The data clearly show that the addition of P(pPD) enhances both the anodic and cathodic overpotentials (but mainly the anodic) and decreases the corrosion current density. These results confirm the suggestion that P(pPD) functions as inhibitor for the acid corrosion of MS electrode. This inhibitor is classified mainly as anodic inhibitor. In all cases, the polarization curves exhibited Tafel type behavior around the corrosion potential, E_{corr} , the electrochemical kinetic parameters associated the polarization curves (i_{corr} , E_{corr} , β_{c} and β_{a}) for MS in 1.0M HCl in the absence and presence of various concentrations of P(pPD) and at different temperatures have been simultaneously determined (in the potential range $\pm 50 \text{ mV}$ from E_{corr}) and are given in Tables (1), (2) and (3).

Table 1. Electrochemical kinetic parameters (i_{corr} , E_{corr} , β_{c} and β_{a}) and inhibition efficiency (IE%) obtained from polarization curves of MS electrode in 1.0 M HCl at 298 K.

P(pPD) conc. (ppm)	i_{corr} (mA cm^{-2})	$-E_{\text{corr}}$ (mV)	β_{c} (mV dec^{-1})	B_{a} (mV dec^{-1})	IE%
Blank	400	692	1.36	0.300	--
2.5	332	675	0.220	1.00	17.00
5.0	296	650	0.400	0.907	26.00
7.5	253.6	634	0.140	0.778	36.60
10.0	206	312	0.100	0.510	48.50
12.5	200	321	0.111	0.612	50.00
15.0	190	316	0.105	0.614	52.50

Table 2. Electrochemical kinetic parameters (i_{corr} , E_{corr} , β_{c} and β_{a}) and inhibition efficiency (IE%) obtained from polarization curves of MS electrode in 1.0 M HCl at 303 K.

P(pPD) conc. (ppm)	i_{corr} (mA cm^{-2})	$-E_{\text{corr}}$ (mV)	β_{c} (mV dec^{-1})	B_{a} (mV dec^{-1})	IE%
Blank	473.2	708	1.43	0.306	--
2.5	410	672	0.226	1.00	13.35
5.0	356	652	0.407	0.907	24.77
7.5	325	641	0.144	0.778	31.32
10.0	271	632	0.104	0.510	42.74
12.5	260	612	0.112	0.612	45.05
15.0	250	610	0.110	0.619	47.17

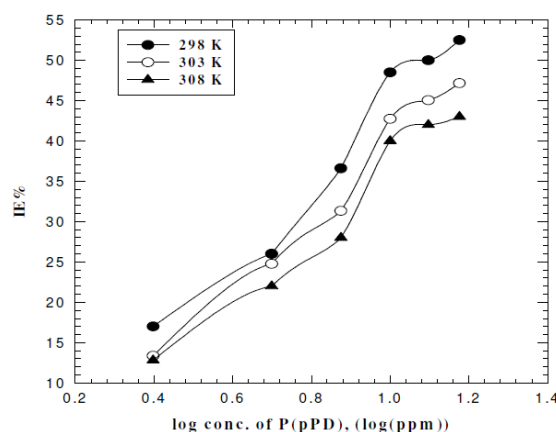
Table 3. Electrochemical kinetic parameters (i_{corr} , E_{corr} , β_c and β_a) and inhibition efficiency (IE%) obtained from polarization curves of MS electrode in 1.0 M HCl at 308 K.

P(pPD) conc. (ppm)	i_{corr} (mA cm ⁻²)	$-E_{\text{corr}}$ (mV)	β_c (mV dec ⁻¹)	B_a (mV dec ⁻¹)	IE%
Blank	500	680	1.48	0.309	--
2.5	436	653	0.201	1.000	12.80
5.0	390	641	0.401	0.901	22.00
7.5	360	623	0.103	0.786	28.00
10.0	300	607	0.109	0.519	40.00
12.5	290	616	0.119	0.619	42.00
15.0	285	614	0.112	0.611	43.00

Since the corrosion rate (CR) is directly related to the corrosion current density [14], the inhibition efficiency, IE%, at different inhibitor concentrations and solution temperatures was calculated from equation [15]:

$$IE\% = \left[1 - \frac{i_{\text{corr}}}{i_{\text{corr}}^0} \right] \times 100 \quad \text{Eq. (2)}$$

where, i_{corr}^0 and i_{corr} are the corrosion current density for uninhibited and inhibited solutions, respectively. The calculated values of IE% are given in Tables (1), (2) and (3). The relation between IE% versus log P(pPD) concentration at the three tested temperature is shown in Fig. (6). According to these data, it is observed that the inhibition efficiency of P(pPD) increases with increasing its concentration but decreases with temperature. It is clear that the weight loss and potentiodynamic polarization techniques gave the same trends of inhibition of P(pPD) and produced nearly the same values of IE%.

**Figure 6.** Relation between IE% and log of the concentration of P(pPD) in 1.0 M HCl at 298, 303 and 308 K for potentiodynamic technique.

Thermodynamic Activation Functions of the Corrosion Process

More information concerning the adsorption mechanism can be gained by the thermodynamic function for the MS corrosion in HCl solution with and without

different concentrations of P(pPD). These functions were obtained by applying the Arrhenius equation [16]:

$$\log(CR) = -\frac{E_a^o}{2.303 RT} + A \quad \text{Eq. (3)}$$

where, E_a^o is the apparent activation energy, A is the pre-exponential factor, T is the temperature and R is the ideal gas constant. An alternative form of Arrhenius equation, [16], is the transition state (Eyring) equation [16]:

$$CR = \frac{RT}{Nh} \exp\left(\frac{\Delta S^o}{R}\right) \exp\left(-\frac{\Delta H^o}{RT}\right) \quad \text{Eq. (4)}$$

where, h is the Planck's constant, N is the Avogadro's number, ΔS^o and ΔH^o are respectively the entropy and the enthalpy of activation.

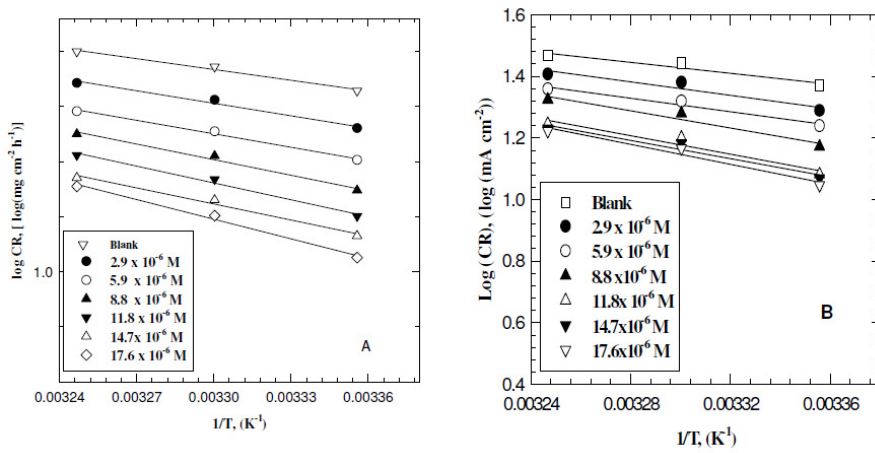


Figure 7. Arrhenius plot of corrosion rate of MS in 1.0 M HCl containing various concentrations of P(pPD). (A) from weight loss and (B) from polarization measurements.

Plotting the relation between logarithmic of the corrosion rate obtained from weight loss and polarization measurements versus 1/T (Arrhenius equation) for MS electrode in 1.0 M HCl containing various concentrations of P(pPD) gave straight lines, as shown in Fig. 7(A) and (B), respectively. The values of apparent activation energy, E_a^o , obtained from the slopes of these lines are given in Table (4).

Plotting the relation $\log(CR/T)$ versus (1/T) for MS in 1.0 M HCl containing various concentrations of P(pPD) should give straight lines with slope of $(-\Delta H^o/2.303R)$ and an intercept of $[(\log(R/Nh)) + (\Delta S^o/2.303R)]$ (transition state equation).

Fig. 8 (A) and (B)) display the plots of $\log(CR/T)$ versus (1/T) from data obtained from weight loss and polarization measurements, respectively. The values of the thermodynamic functions ΔH^o and ΔS^o were obtained and are listed in Table (4).

The data infer that the values of E_a^o , ΔH^o and ΔS^o of the dissolution of MS in 1.0 M HCl solution in the presence of P(pPD) are higher than those in the blank acid solution. The activation thermodynamic parameters of the corrosion process

enhance with increasing the inhibitor concentration, indicating that more energy barrier for the corrosion reaction in the presence of inhibitor is attained [17].

Table 4. Thermodynamic activation functions of MS dissolution in 1.0M HCl in the absence and presence of different concentrations of P(pPD) obtained from weight loss and polarization data by applying Arrhenius and Transition state plots.

P(pPD) conc.(M)x10 ⁻⁶	Weight loss			Polarization		
	E _a ^o (kJ mol ⁻¹)	ΔH ^o (kJ mol ⁻¹)	ΔS ^o (J mol ⁻¹ K ⁻¹)	E _a ^o (kJmol ⁻¹)	ΔH ^o (kJmol ⁻¹)	ΔS ^o (J mol ⁻¹ K ⁻¹)
Blank	12.53	11.24	-182.07	17.08	14.55	-187.81
2.9	14.49	11.99	-180.54	18.32	18.32	-161.20
5.9	15.55	13.04	-178.05	18.55	18.55	-159.28
8.8	18.02	15.51	-170.77	24.28	24.28	-142.05
11.8	19.51	16.98	-166.75	25.27	26.23	-140.14
14.7	21.06	17.19	-163.11	25.89	26.77	-138.22
17.6	22.73	20.20	-157.37	28.47	28.47	-129.22

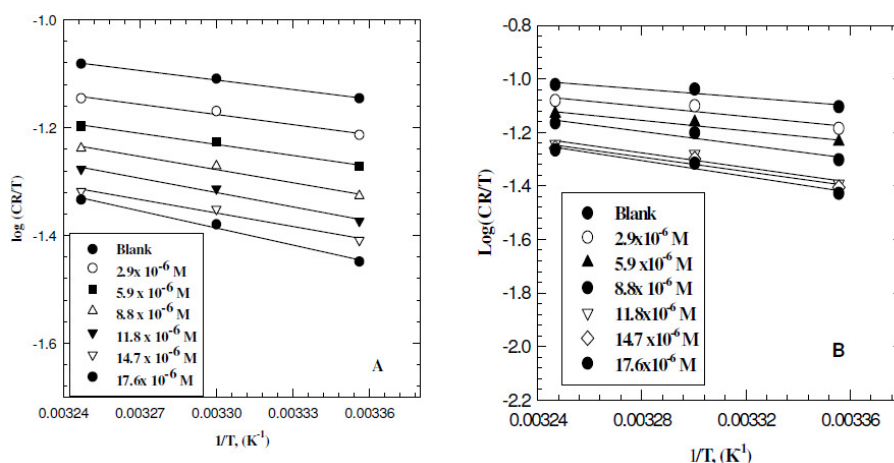


Figure 8. Transition state plot of corrosion rate of MS in 1.0 M HCl containing various concentrations of P(pPD). (A) From weight loss and (B) from polarization measurements.

Adsorption Isotherms and Thermodynamic Functions of Adsorption Process

Langmuir isotherm has been tested with the experimental data obtained from both weight loss and polarization measurements for MS electrode in 1.0 M HCl in the presence of different concentrations of P(pPD) and temperatures.

In all cases, it is observed that the linear regression between C_{inh} / θ and C_{inh} , calculated by the computer, and the slope and the linear correlation coefficient (r^2) are close to unity, as shown in Fig. (9) and (10), respectively; the correlation coefficient r^2 is higher than 0.99 [20], reflecting adsorption of P(pPD) species on the electrode surface and applicability of Langmuir isotherm model (c.f. Table (5)).

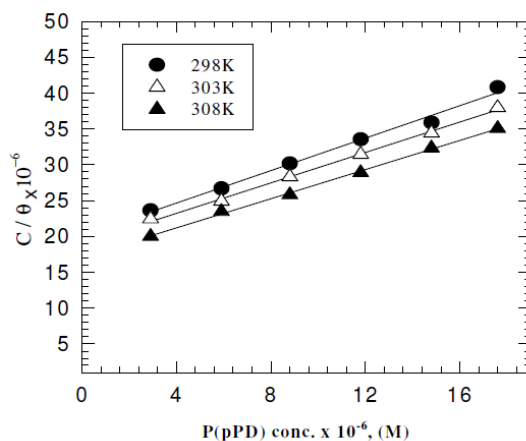


Figure 9. C_{inh} / θ versus C_{inh} for MS in 1.0 M HCl data obtained from weight loss technique.

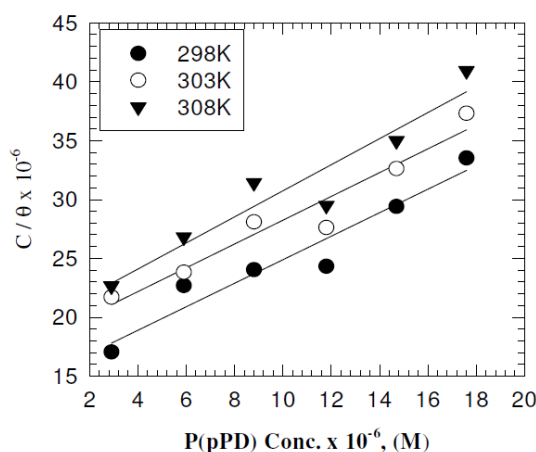


Figure 10. C_{inh} / θ versus C_{inh} for MS in 1.0M HCl data obtained from polarization technique.

The adsorption isotherm relationship of Langmuir is represented using the following equation [21]:

$$\frac{\theta}{1 - \theta} = K_{ads} C_{inh} \quad \text{Eq. (5)}$$

where, K_{ads} is the adsorption-desorption equilibrium constant.

Table 5. Data obtained from Fig. (9) and (10).

Temp.(K)	298K	303K	308K	298K	303K	308K
Slope	1.31	1.05	1.02	0.99	1.01	1.11
r^2	0.991	0.997	0.998	0.995	0.996	0.991

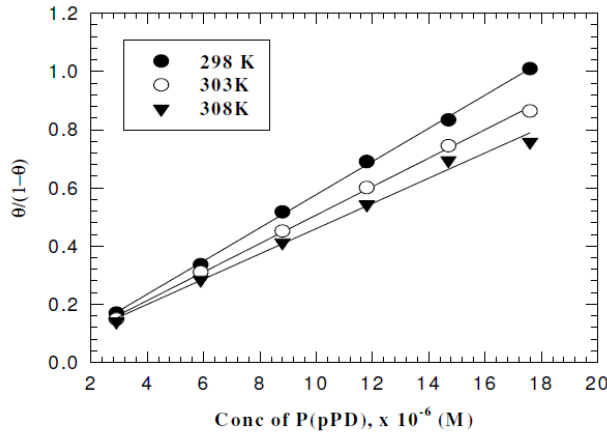


Figure 11. Langmuir isotherm for MS in 1.0 M HCl in the presence of different concentrations of P(pPD) and temperatures. Data from weight loss technique.

However, the relation between of $(\theta / 1- \theta)$ against C_{inh} gave straight lines, as shown in Fig. (11) and (12). These results show that the fitting of corrosion data is in agreement with Langmuir's isotherm [21] and confirm the assumption that the action of the inhibitor is due to its adsorption at the metal/solution interface. The equilibrium adsorption constant, K_{ads} , for the adsorption of the inhibitor at MS electrode surface at $T=298, 303$ and 308 K were obtained from the slopes of these straight lines. The free energies of the inhibitor adsorption, ΔG°_{ads} , were calculated from the equation [22]:

$$K_{ads} = \frac{1}{55.5} \exp \frac{-\Delta G^{\circ}_{ads}}{RT} \quad \text{Eq.(6)}$$

where, 55.5 is the molar concentration of water.

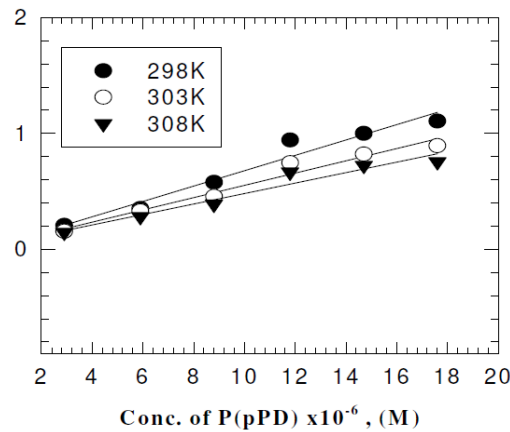


Figure 12. Langmuir isotherm for MS in 1.0 M HCl in the presence of different concentrations of P(pPD) and temperatures. Data from polarization technique.

Table 6. Thermodynamic parameters of adsorption of P(pPD) on MS electrode surface in 1.0 M HCl solution. Data from weight loss technique.

Temp , (K)	$K_{ads} \times 10^{-6}$	ΔG_{ads}° (kJ mol ⁻¹)	ΔH_{ads}° (kJ mol ⁻¹)	ΔS_{ads}° (J mol ⁻¹ K ⁻¹)
298	0.056	-37.04	-46.41	-143.97
303	0.049	-37.32		
308	0.043	-37.60		

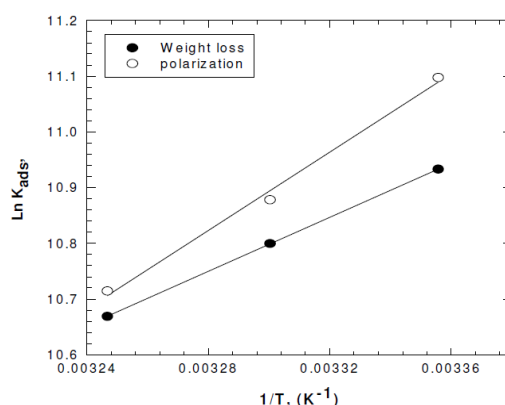
The integrated version of the Van Hoff equation [22] is:

$$\ln K_{ads} = \frac{-\Delta H_{ads}^{\circ}}{RT} + \text{constant} \quad \text{Eq. (7)}$$

The calculated values of K_{ads} using data obtained from weight loss and polarization measurements are given in Tables (6) and (7), respectively. It is clear that the values of K_{ads} are relatively small and decrease with rise of temperature. This behavior indicates that this inhibitor is physically adsorbed on the metal surface and the strength of adsorption decreases with temperature. Moreover, it is seen that there is a good agreement between the values of K_{ads} obtained from the two methods used. The average thermodynamic functions (ΔH_{ads}° and ΔS_{ads}°) for P(pPD) adsorption on metal surface were calculated using equations (7) and (8), respectively, since plotting $\ln K_{ads}$ against $1/T$ gave straight lines, as shown in Fig. (13).

Table 7. Thermodynamic parameters of adsorption of P(pPD) on MS electrode surface in 1.0 M HCl solution. Data from polarization technique.

Temp , (K)	$K_{ads} \times 10^{-6}$	ΔG_{ads}° (kJ mol ⁻¹)	ΔH_{ads}° (kJ mol ⁻¹)	ΔS_{ads}° (J mol ⁻¹ K ⁻¹)
298	0.066	-37.44	-67.34	-211.27
303	0.053	-37.52		
308	0.045	-37.72		

**Figure 13.** Relation between $\ln K_{ads}$ and $1/T$ for MS electrode in 1.0 M HCl.

The calculated values of ΔG_{ads}° , ΔH_{ads}° and ΔS_{ads}° obtained from weight loss and polarization methods are given in Tables (6) and (7), respectively. It seems that the thermodynamic functions of the adsorption process obtained from the two methods are parallel and in a good agreement. The calculated values of ΔG_{ads}°

are low and negative, suggesting that the nature of this inhibitor adsorption is mainly physisorption and spontaneous [22-25]. It is usually accepted that the value of $\Delta G^{\circ}_{\text{ads}}$ around -20 kJ mol^{-1} or lower indicates the electrostatic interaction between charged metal surface and charged organic inhibitor in the bulk of the solution [26], while those around -40 kJ mol^{-1} or higher involve charge sharing transfer between the metal surface and the organic inhibitor [27]. The negative values of $\Delta H^{\circ}_{\text{ads}}$ indicate that the adsorption is an exothermic process [18]. The magnitude of the values of $\Delta H^{\circ}_{\text{ads}}$ and $\Delta S^{\circ}_{\text{ads}}$ is characteristic of the occurrence of replacement process during adsorption [28, 29].

Conclusion

The tested P(p-PD) compound inhibits the corrosion of mild steel in HCl media. The addition of P(p-PD) does not change the mechanism of either mild steel dissolution or hydrogen evolution reaction. P(p-PD) acts as a mixed type inhibitor, but predominantly as an anodic one. The inhibition efficiency value increases with the inhibitor concentration and decreases by increasing acid concentration and temperature. The corrosion inhibition of P(p-PD) can be interpreted by a simple blocked fraction of the electrode surface related to the adsorption of the inhibitor species, according to a Langmuir isotherm on the MS and mainly the adsorption process is spontaneous and exothermic physisorption. The results obtained from polarization curves and the weight loss data are in reasonably good agreement.

References

1. P. Zhao, Q. Liang, Y. Li, *Appl. Surf. Sci.* 252 (2005) 1596.
2. A.M.S. Abdennabi, A.I. Abdulhadi, and S. Abu-Orabi, *Anti-Corros. Met. Mater.* 45 (1998)103.
3. K.F. Khaled, *Electrochim. Acta* 48 (2003) 2493.
4. K. Emregul, O. Atakol, *Chem. Phys.* 82 (2003) 188.
5. D.M. Lenz, M. Delamar, C.A. Ferreira, *J. Electroanal. Chem.* 54 (2003) 35.
6. M. El Azhar, M. Traisnel, B. Mernari, L. Gengembre, F. Bentiss, M. Lagrenee, *Appl. Surf. Sci.* 185 (2002) 197.
7. M. Ajmal, A.S. Mideen, M.A. Quraishi, *Corros. Sci.* 36 (1994) 79.
8. S. Arab, E.E.A. Noor, *Corrosion* 49 (1993) 122.
9. M.A. Quraishi, R. Sardar, *Mater. Chem. Phys.* 78 (2002) 425.
10. S. Arab, E.E.A. Noor, *Corrosion* 49 (1993) 122.
11. Z.D. Stankovic, M. Vukovic, *Electrochim. Acta* 41 (1996) 2529.
12. S.M. Sayyah, M.M. El-Deeb, S.M. Kamal, R.E. Azooz, *Appl. Poly. Sci.* 117 (2010) 943.
13. S.S. Abd El Rehim, H.H Hassan, M.A. Amin, *Mat. Chem. Phys.* 78 (2002) 337.
14. M.A. Amin, S.S. Abd El Rehim, E.E.F. El-Sherbini, R.S. Bayoumi, *Inter. J. Electrochem. Sci.* 3 (2008) 199.
15. M.A. Amin, *J. Appl. Electrochem.* 36 (2006) 215.

16. J.O'M. Bockris, A.K.N. Reddy, "Modern Electrochemistry" Vol. 2, Platinum Press, N.Y. 1977.
17. F. Mansfeld, "Corrosion Mechanism" p. 119, Marcel Dekker, N.Y. 1987.
18. J. March: Advanced Organic Chemistry: 3rd. ed., Will Eastern, New Delhi, 1988.
19. E. McCaffery, "Corrosion Control by Coating", Science Press, Princeton, 1979.
20. Y. Yan, W. Li, L. Cai and B. Hou, *Electrochim Acta* 53 (2008) 5953.
21. I. Langmuir, *J. Am. Chem. Soc.* 39 (1917) 1848.
22. D. Do, "Adsorption Analysis: Equilibria and Kinetics", Imperial College Press, London, 1998.
23. E. Khamis, I. Mellucci, R.M. Lantianison, E.S.H. El-Ashry, *Corros. Sci.* 47 (1991) 677.
24. F.M. Donahue, k. Noble, *J. Electrochem. Soc.* 112 (1965) 886.
25. P.W. Atkins, Physical Chemistry, 6th. Ed., Oxford Univ. Press 1999, p857.
26. H. Keles, M. Keles, I. Dehri, O. Serindag, *Colloids surf. A: Physicochem. Eng. Aspects* 320 (2008)138.
27. A.K. Singh, M.A. Quraishi, *Corrosion Sci.* 51 (2009) 2752.
28. B.A. Abdel Nabey, E. Khamis, M. Sh. Ramadan, A. El-Gidy, 8th Eur. Symp. Corros. Inhibitors, Ann Univ. Ferrara, NS Sez. 10 (1995) 299.
29. M.J. Lampinen and M. Fomino, *J. Electrochem. Soc.* 140 (1993) 3537.